Excitation Modes in Multiferroics [1]

E.I. Kats, A.Cano

Laue-Langevin Institute, Grenoble, France
L.D.Landau Institute for Theoretical Physics RAS, Moscow, Russia

20th June 2008

[1] Phys. Rev. B (2008)

Early works on M.E. effect:

- P.Curie (1894): First proposal on the effect;
- Perrier (1923): Claim to have observed the effect in iron;
- Piccard (1924): Suggest the impossibility of the effect;
- Szivessy (1925): Expects to find the effect in liquid crystals but his experiments show no results;
- Perrier, Borel (1925): Find no effect in nickel and suggest that their 1923 experiments on iron were wrong;
- Debye (1926): Suggests the effect is impossible;
- Huber (1926): Studies *NO* etc, and finds no effect;
- Van Vleck (1932): Devotes a section of his book to the reasons why no m.e. effect can exist;
- Condon (1937): Gives the first quantum mechanical description of the effect;
- Landau, Lifshits (1957): Show that the m.e. effect should exist in magnetic crystals;
- Dzyaloshinskii (1959): Shows that the chromium oxide has a magnetic symmetry which allows the effect, Astrov (1960): First successful observation.

All forms of ferroics:

Time \ Space	Invariant	Change
Invariant	Ferroelastic 	Ferroelectric 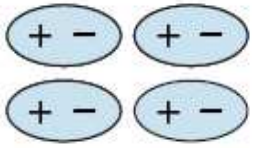
Change	Ferromagnetic 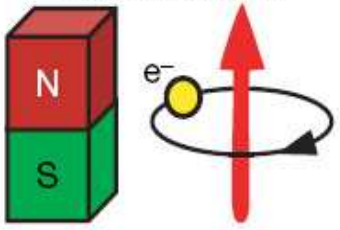	Ferrotoroidic 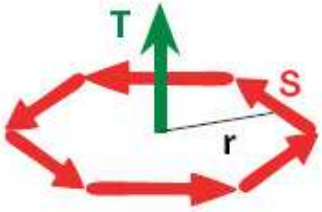

Materials which combine two or more ferroic properties are known as multiferroics

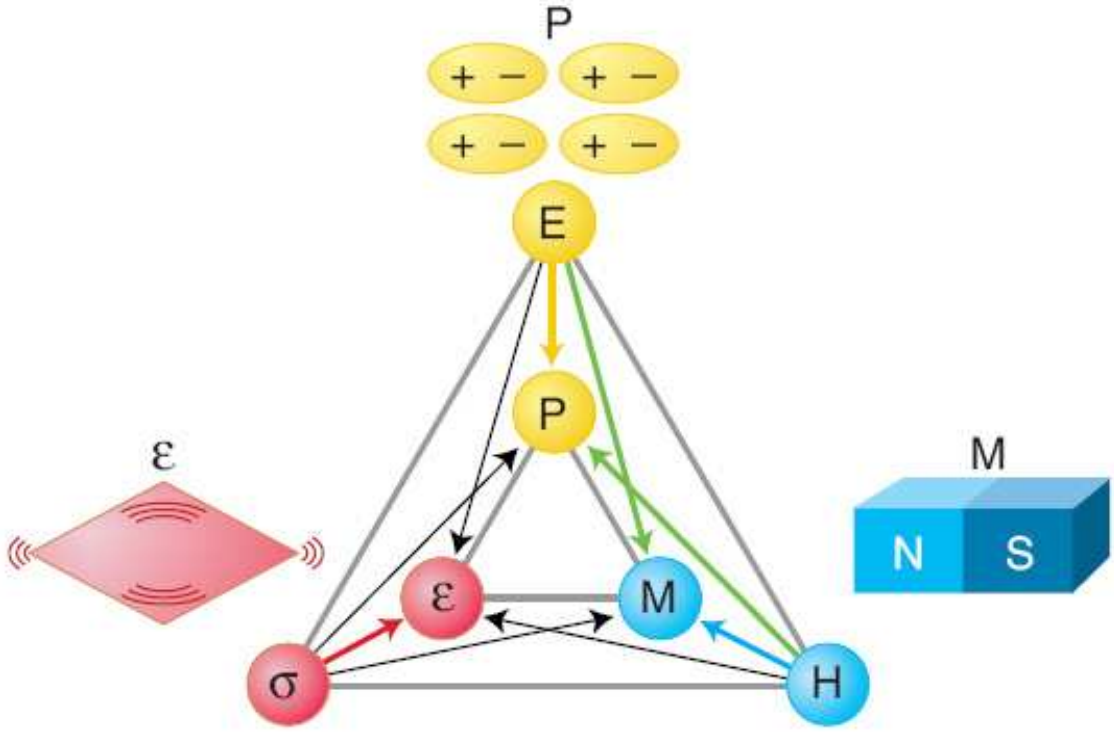

Figure: Phase control in multiferroics.

Revival of interest to multiferroics

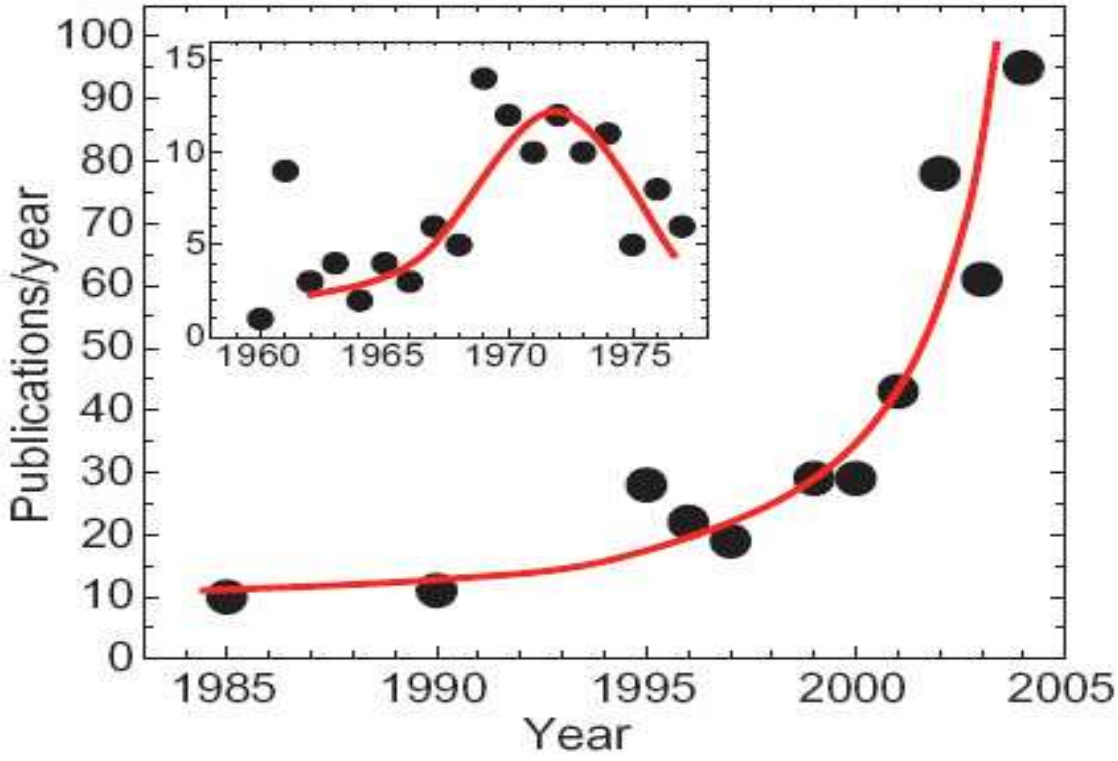

Figure: Publications per year.

Ferroics are materials

- with a spontaneous magnetic polarization that can be reversed by a magnetic field (applications: memory devices);
- with a spontaneous electric polarization that can be switched by an electric field (ferro-pyro-piezo-electrics, but not reverse; applications: sensors);
- ferroelastics, where changes of electric polarization is accompanied by deformation (applications: sonor detectors, electrocaloric effect: $\Delta T = T_1 - T_2 \simeq [P_1^2(E) - P_2^2(0)]$;
- ferrotoroidicity **t**.

Toroidal moment:

- $$\mathbf{t} = \frac{1}{c}\int (\mathbf{r}(\mathbf{rj}) - 2\mathbf{r}^2\mathbf{j})\mathbf{d}^3\mathbf{r}$$

  It is identity for $\mathbf{j}(\mathbf{r}) = c\nabla \times \nabla \times \delta(r)\mathbf{t}$, i.e. it represents an elemental toroidal moment centered at the origin.
- The toroidal moment couples to the curl of the magnetic field (energy $\propto \int d^3 r \mathbf{jA}$) such that the lowest energy takes place when the toroidal moment is aligned parallel to the curl.
- Only the transverse part $\mathbf{j}_\perp$ (i.e., $\nabla \mathbf{j}_\perp = 0$ and $\mathbf{j}_\perp = c\nabla \times \mathbf{m}$) contributes to $\mathbf{t}$:

  $$\mathbf{t} = \frac{1}{2}\int [\mathbf{r} \times \mathbf{m}] d^3 r$$

  If the magnetization density can be represented by localized moments $\{\mathbf{m}_\alpha\}$, $\mathbf{t} = (1/2)\sum_\alpha \mathbf{r}_\alpha \times \mathbf{m}_\alpha$.

For non-localized magnetization its un-compensated part cannot break space inversion symmetry, thus it results in a perfect separation of dipolar and toroidal contributions.

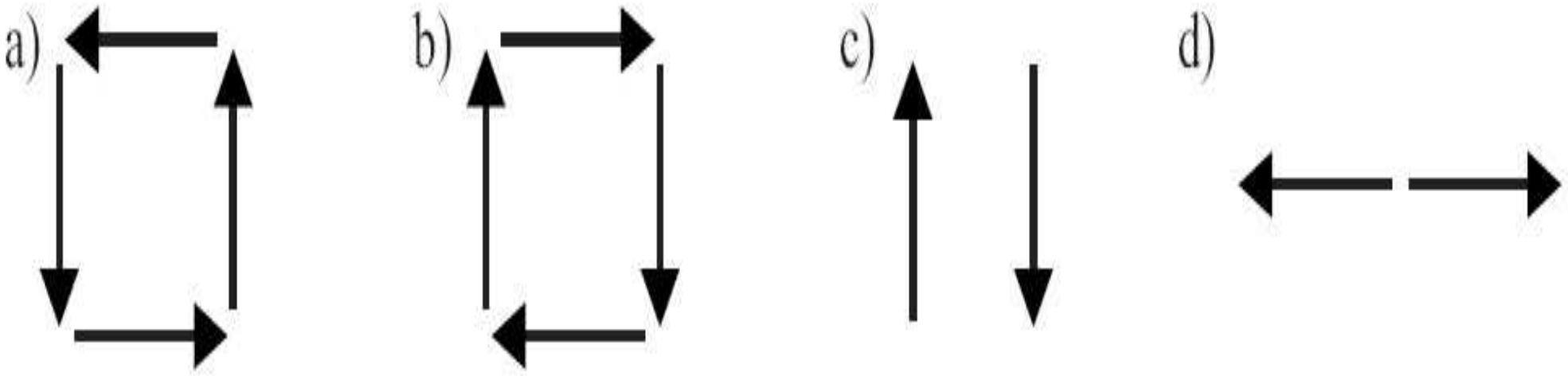

a), and *b*) have equal and opposite $\mathbf{t} = \pm am\hat{z}$.
A.F. in *c*) has $\mathbf{t} = -(1/2)am\hat{z}$, whereas in *d*) $\mathbf{t} = 0$.

Toroidal moment $\equiv$ Magnetic vortex:

$$\mathbf{M} = M[\cos(n\phi + \phi_0)\mathbf{e_1} + \sin(\mathbf{n}\phi + \phi_\mathbf{0})\mathbf{e_2}]$$

where $\phi = \tan^{-1}(y/x)$.
This distribution yields to electric dipole polarization

$$\propto [\mathbf{M}(\nabla\mathbf{M}) - (\mathbf{M}\nabla)\mathbf{M}]$$

It has quantized electric (!) charge located at the vortex core:

$$q_1 = 2\pi\gamma\chi_E M^2$$

Thus applied electric field will pull vortices and anti-vortices in opposite directions.

More on toroidal moments: Magnetic moment distribution can be decomposed into totally compensated part

$$\mathbf{m}_\alpha^0 \equiv m_\alpha - \frac{\mathbf{m}}{N}$$

and an un-compensated, ferromagnetic part

$$\tilde{\mathbf{m}}_\alpha \equiv \frac{\mathbf{m}}{N}$$

Only differences in toroidal moment have any physical signifi cance.

Decomposition of localized moments into compensated and ferromagnetic components

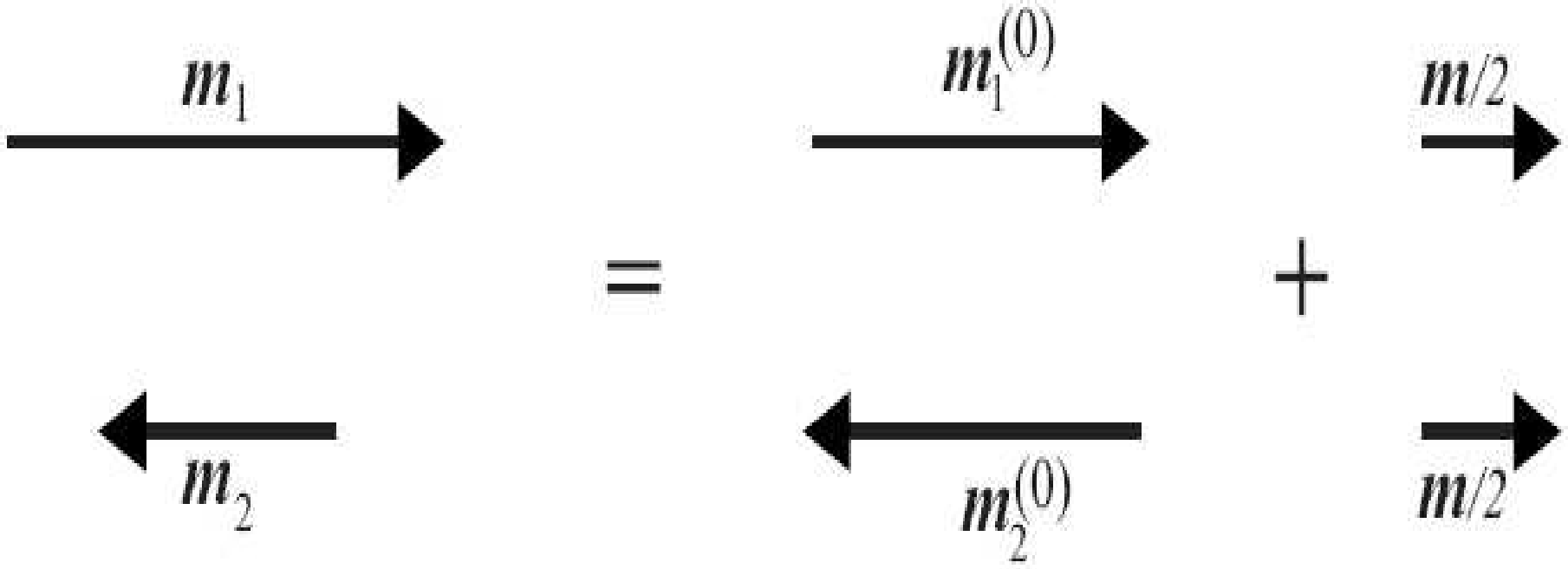

More on toroidal moments:

- $\mathbf{P} \times \mathbf{M}$ has the same time and space reversal symmetry as $\mathbf{t}$ but generally it can not describe a toroidal moment (e.g., for the compensated part when $\mathbf{M} = 0$);
- Similarly for the un-compensated part $\Delta\tilde{\mathbf{t}} = (1/2)\Delta\bar{\mathbf{R}} \times \mathbf{m}$, the average displacement $\Delta\bar{\mathbf{R}}$ is not proportional to $\mathbf{P}$.

One may introduce also electric toroidal moments $\mathbf{g} \propto \sum_i \mathbf{r}_i \times \mathbf{p}_i$. However the vector **g** is fundamentally different from the magnetic toroidal moment $< \mathbf{t} > \propto < \mathbf{P} \times \mathbf{M} >$, since it is both time- and space-inversion symmetric (however, **g** might be used to characterize ferroelastics!).

Why chirality?

Chirality in magnetic solids allows the mixing of electronic, optical, magnetic and structural properties.

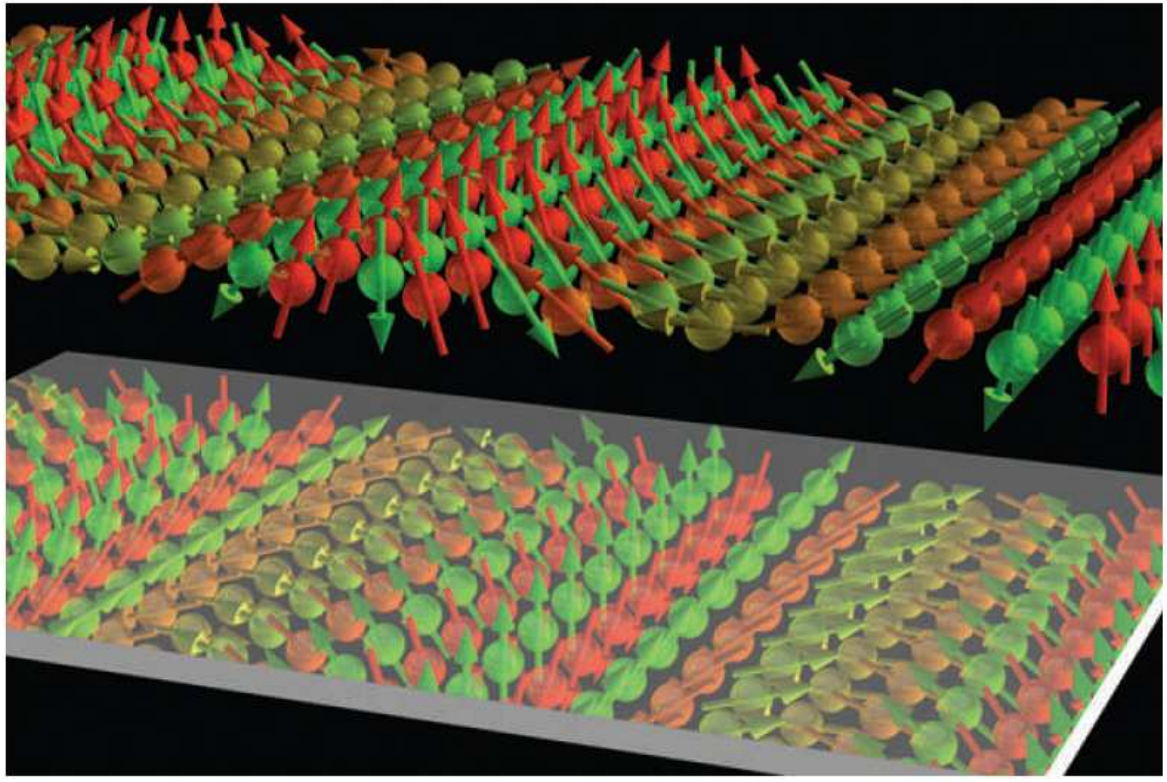

Why is it difficult to find materials that are multiferroics?

- Most of ferroelectrics are transition metal oxides (empty *d* shells). These positively charged ions like to form ”molecules” with neighboring negative oxygen ions: virtual hopping of electrons;
- Magnetism requires partially filled *d* shells;
- Thus in the proper ferroelectrics both orders should be associated with different ions - the coupling is weak;
- Improper ferroelectrics: charge carriers become localized and form periodic superstructures. When charges order in non-centrosymmetric fashion - they induce electric polarization;
- Improper ferroelectricity puts lower constraints on the coexistence with magnetism.

- Mechanism of F.E. ”molecular bonding” is based on the virtual hopping of electrons from the filled oxygen shell to the empty shell of a transition metal ion.
- Exchange interaction results also from the virtual hopping of electrons between ions.

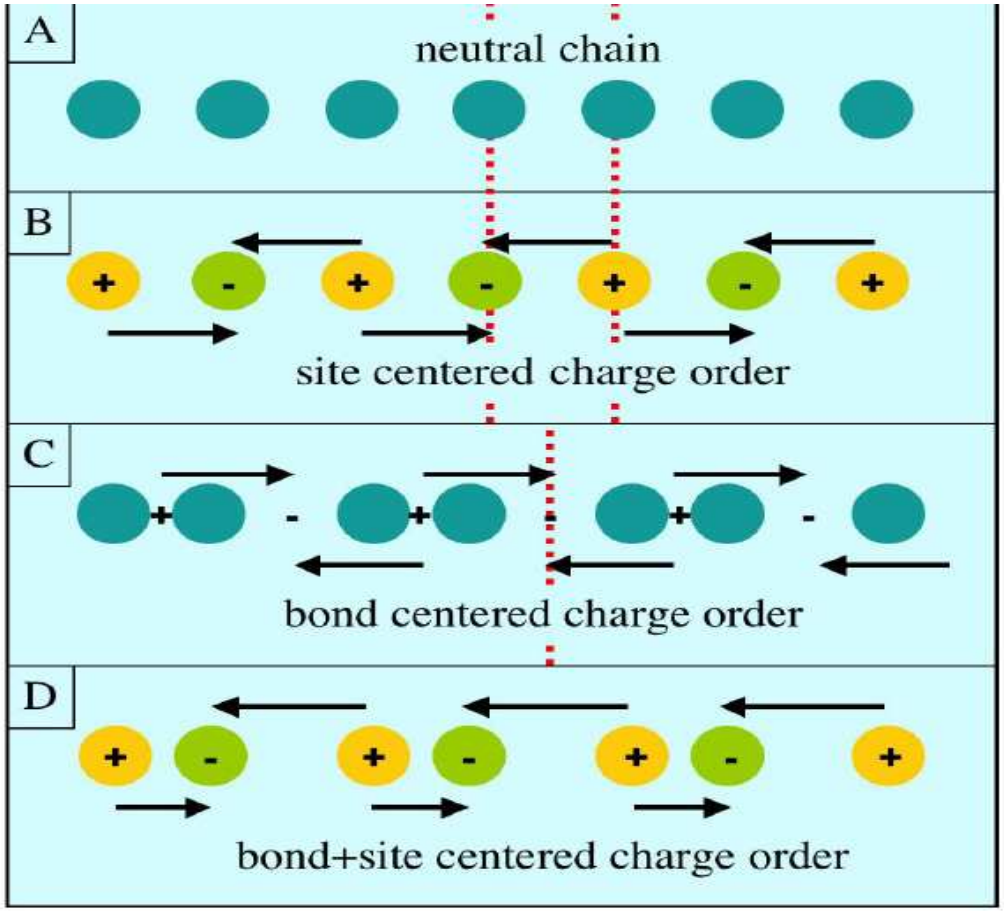

Figure: Site- and Bond- ordering mechanisms of F.E.

Ferroelectric Materials:

- Proper ferroelectrics:
- Inversion symmetry breaking by:
- Covalent bonding between $3d^0$ transition metal (*Ti*) and oxygen ($BaTiO_3$);
- Polarization of $6s^2$ lone pair of *Bi* or *Pb* ($BiMnO_3$, $BiFeO_3$);
- Improper:
- Geometric ferroelectrics (structural ordering in K_2SeO_4, hexagonal $RMnO_3$);
- Electronic ferroelectrics (charge ordering in $LuFe_2O_4$);
- Magnetic ferroelectrics (magnetic ordering in orthorhombic $RMnO_3$, $RMnO_5$, $CoCr_2O_4$).

M.E. terms in free energy:

$$\alpha_{ij} < P_i >< M_j > + \beta_{ijk} < P_i >< M_j M_k >$$

$-P^2M^2$ term does not induce ferroelectricity
(over-compensated by a polar lattice distortion $\propto +P^2$.

- Linear M.E. effect vanishes above the Curie temperature, whereas the quadratic term $\propto < M^2 >$ remains finite well above;
- $\chi^2_{M.E.} \leq \chi_M \chi_E$ but that ignores indirect coupling, e.g., through the strain.

Why it is interesting?

- Usual atomic-level mechanisms driving ferromagnetism and ferroelectricity are mutually exclusive: empty and simultaneously partially filled transition metal orbitals.
- However, multiferroics have not only properties of parents. Interactions between magnetic and electric polarizations lead to additional functionality, e.g., large M.E. effects observed in perovskites and hexagonal manganites.
- Spin excitations - electromagnons, which can be excited by a.c. electric field.
- Dynamical effects: in conventional ferroelectrics - softening of optical phonons results in divergent ϵ. Mixing of magnons with optical phonons makes it is possible to see magnons in optical absorption experiments (**in ordinary magnets it occurs only through magnetic dipole coupling of the light, magnetic resonance, and it is much weaker).**

Photo-excitation of magnons:

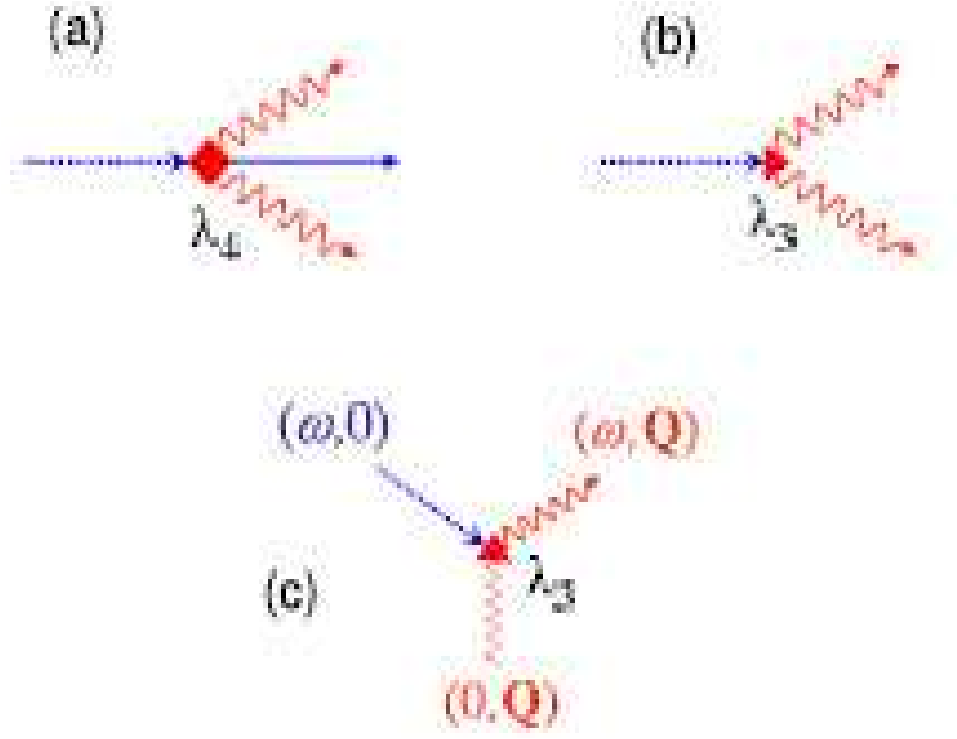

Figure: (a) two magnons and one phonon via 4-th order m.e. interaction; (b) two magnons via 3-d order m.e. coupling; (c) photon with the frequency ω and $q = 0$ scatters off the static spin modulation with the wave vector Q producing a magnon with the same Q and the frequency ω.

Electromagnons:

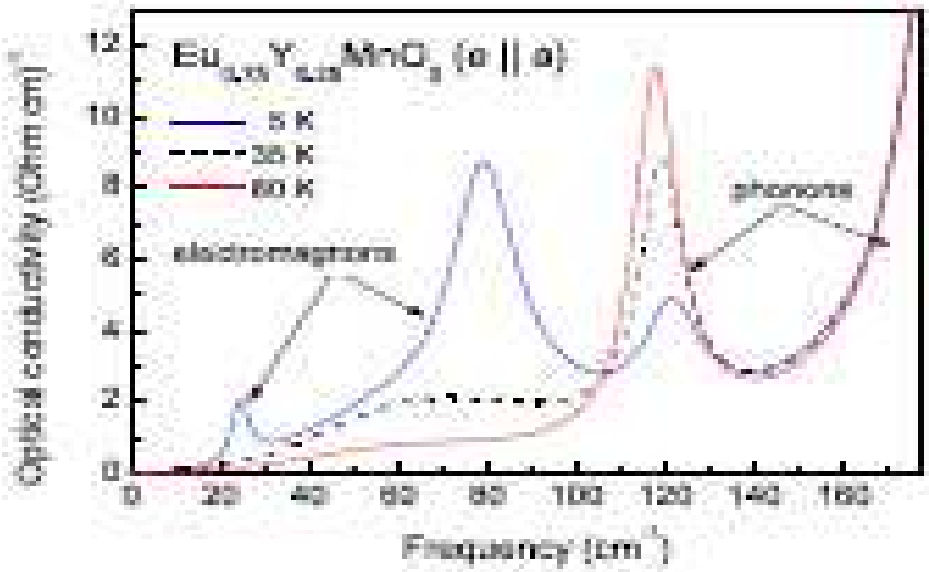

Figure: Optical conductivity data in the ferroelectric (blue), the SDW (dashed), and the paramagnetic (red) phases. Electromagnon band consists of a broad background and two peaks.

Pair Dzyaloshinskii - Moria interaction:

When the spins on the adjacent sites are canted, the horizontal mirror-plane symmetry is lost, and polarization can be generated along the vertical direction.

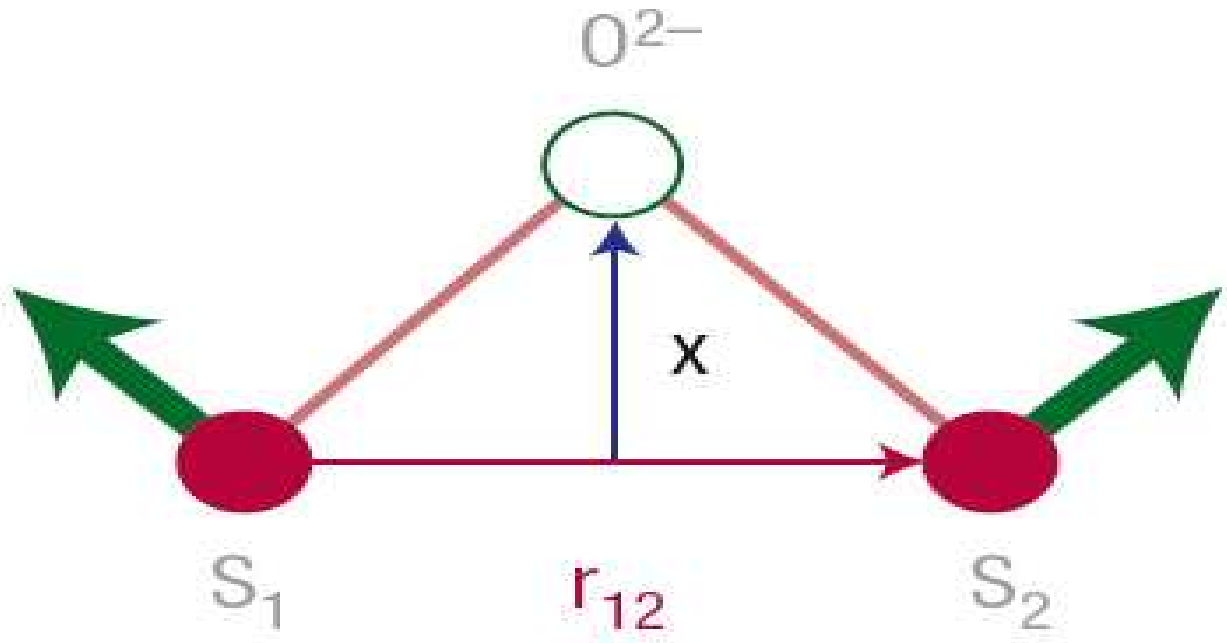

Figure: DM interaction.

Polarization due to DM interaction:

Exchange between spins of the transition metal ions is mediated by ligands (e.g., oxygen ions), and the Dzyaloshinskii vector $\propto \mathbf{x} \times \mathbf{r}$, where **r** is a unit vector along the line connecting the magnetic ions, and **x** is the shift of the oxygen ion from this line.

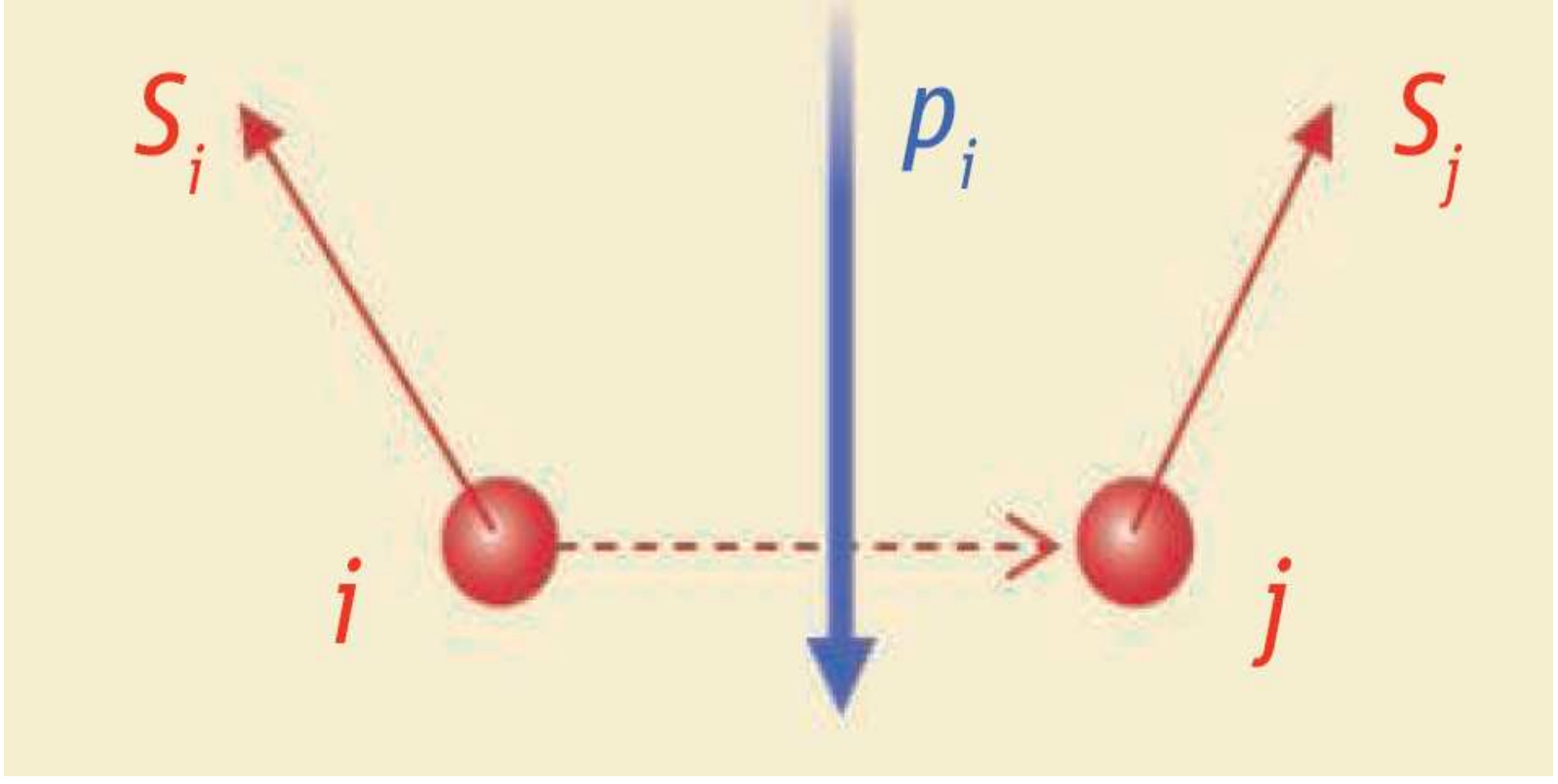

Figure: DM induced polarization.

Collective DM induced polarization:

Because in the spiral state the vector product $\mathbf{S}_n \times \mathbf{S}_{n+1}$ has the same sign for all pares, the DM interaction pushes negative oxygen ions in one direction perpendicular to the spin chain formed by positive ions, thus inducing **P**.

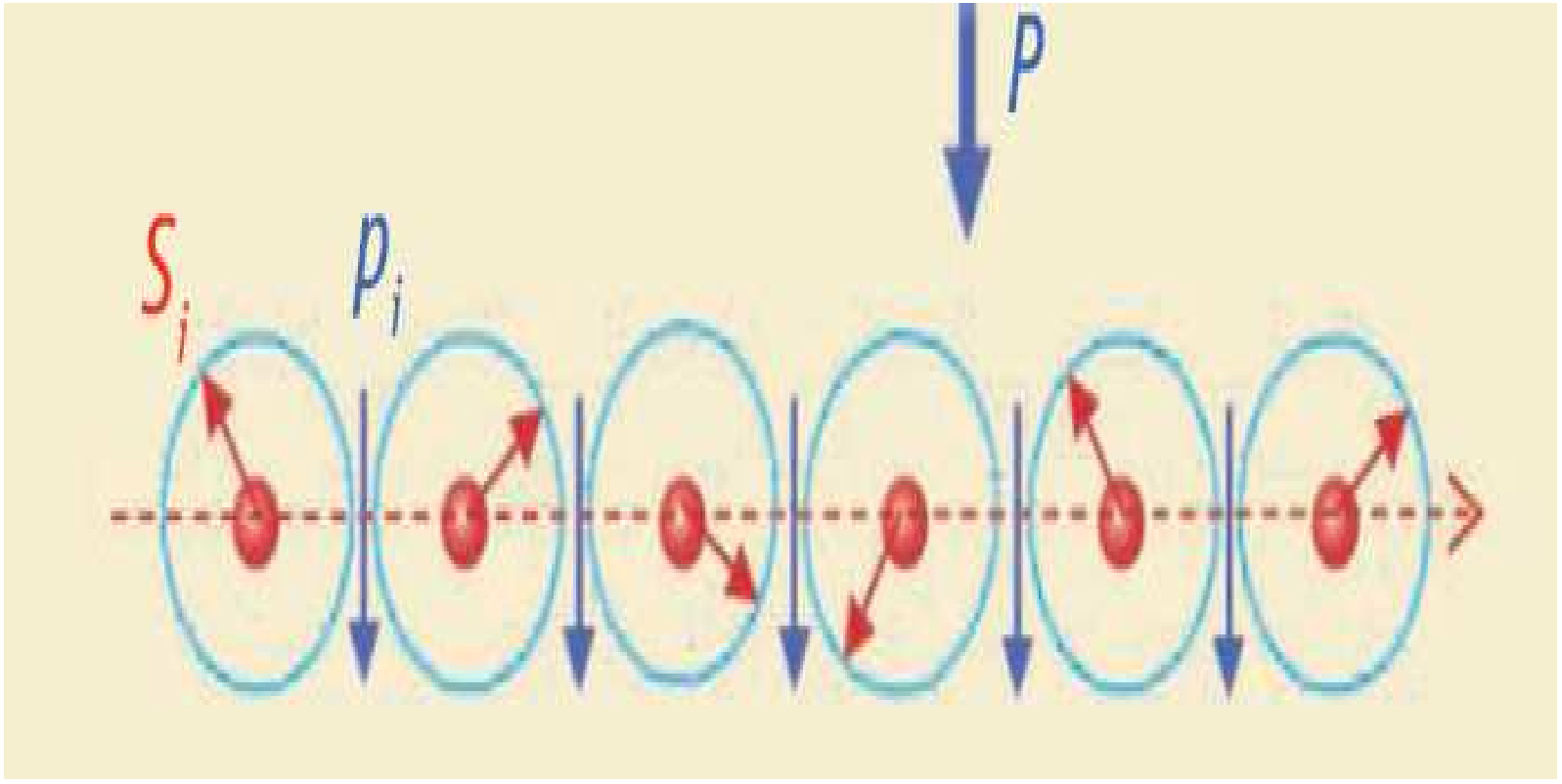

Figure: DM induced polarization.

Non-uniform magnetization:

$$-f_1\mathbf{PM}(\nabla\mathbf{M}) - f_2\mathbf{P}[\mathbf{M}\times[\nabla\times\mathbf{M}]]$$

Only for uniform ferroelectric polarization $\bar{\mathbf{P}}$ it is reduced to

$$-\frac{f_1+f_2}{2}\bar{\mathbf{P}}(\mathbf{M}(\nabla\mathbf{M}) - (\mathbf{M}\nabla)\mathbf{M})$$

$$f_{kl,ij} = S_{kl,ij} + A_{kl,ij}$$

where

$$2S_{kl,ij} = (f_1 - f_2)(\delta_{ki}\delta_{lj} + \delta_{kj}\delta_{li}) + 2f_2\delta_{kl}\delta_{ij}$$

and

$$2A_{kl,ij} = (f_1 + f_2)(\delta_{ki}\delta_{lj} - \delta_{kj}\delta_{li})$$

Clearly $f_1 = -f_2$ yields to a pure symmetric coupling but no non-trivial pure antisymmetric coupling!

”Flexoelectric” polarization:

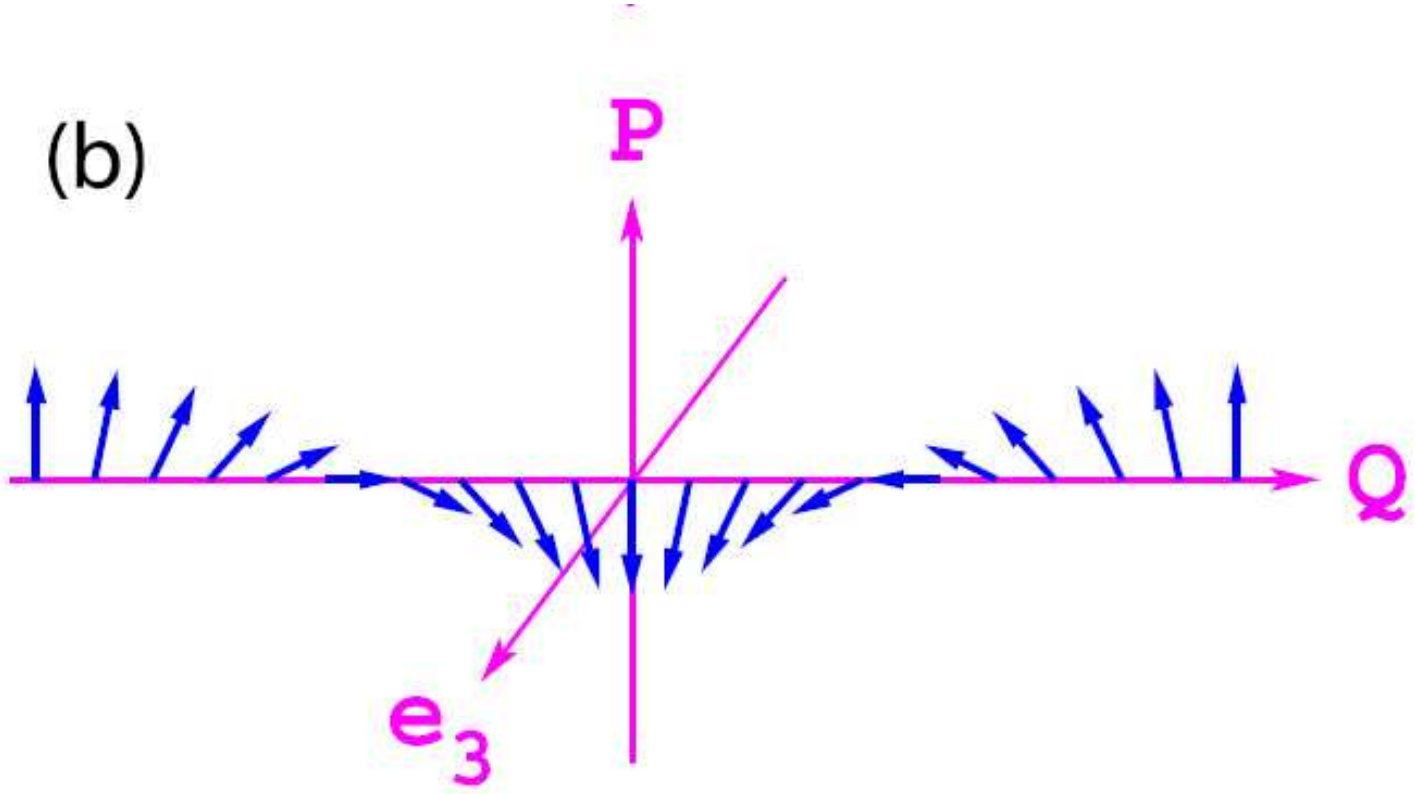

Multiferroics with $\bar{\mathbf{P}} \neq 0$:

- M.E. coupling term

$$F_{ME} = \gamma \mathbf{P}[\mathbf{M}(\nabla \mathbf{M}) - (\mathbf{M}\nabla)\mathbf{M}]$$

- Electric part

$$F_E = \frac{P^2}{2\chi_E}$$

- Thus

$$\mathbf{P} = \gamma \chi_E [\mathbf{M}(\nabla \mathbf{M}) - (\mathbf{M}\nabla)\mathbf{M}]$$

A few examples:

- Conical cycloidal spiral:

$$\mathbf{M} = M_1 \mathbf{e_1} \cos(\mathbf{Qr}) + M_2 \mathbf{e_2} \sin(\mathbf{Qr}) + M_3 \mathbf{e_3}$$

where

$$\bar{\mathbf{P}} = \frac{1}{V} \int d^3 r \mathbf{P} = \gamma \chi_E M_1 M_2 [\mathbf{e_3} \times \mathbf{Q}]$$

- Two non-collinear SDWs with equal **Q**

$$\bar{\mathbf{P}} = \gamma \chi_E M_1 M_2 \sin(\phi_2 - \phi_1) [\mathbf{Q} \times [\mathbf{a_1} \times \mathbf{a_2}]]$$

More examples:

- Magnetic textures: Bloch DW $\bar{\mathbf{P}} = 0$, Neel DW

$$\mathbf{M} = M(\cos(\phi(x))\mathbf{e_1} + \sin(\phi(x))\mathbf{e_2}$$

- Polarization

$$\int_{-\infty}^{+\infty} \mathbf{P}dx = \gamma\chi_E M^2[\phi(+\infty) - \phi(-\infty)]$$

Landau model:

- Magnetic free energy:

$$F_M = \sum_i \frac{a_i}{2} M_i^2 + \frac{b}{4} M^4 + c\mathbf{M}(\nabla^2 + Q^2)^2\mathbf{M}$$

- assuming $a_x < a_y < a_z$, sinusoidal SDW occurs at T_S when, $a_x(T_S) = 0$, and helicoidal structure at

$$T_H = T_S - \frac{3(a_y - a_x)}{2\alpha}$$

  if $a_x = \alpha(T - T_S)$.

- Polarization

$$P_y = \alpha\gamma\chi_E Q[(T_H - T)(T_S + (a_y - a_x)/(2\alpha) - T)]^{1/2}$$

Behavior in magnetic field:

- In zero field spin rotates in the $x-y$ plane and $\mathbf{P}||$ to y;
- Magnetic field in the x direction suppresses the polarization;
- While H_y orients **P** in the z-direction.

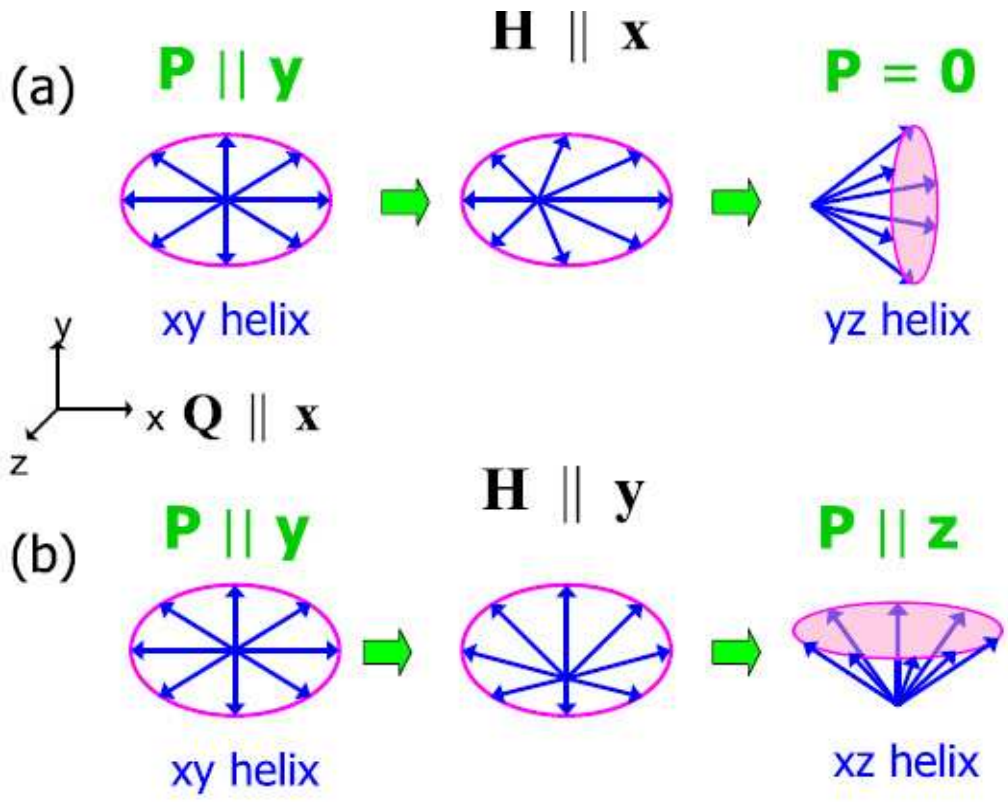

To the same point in words:

m_3, **q**, and **P** are always in mutually orthogonal directions. If the direction of **H** is reversed, reversing $m_3 \rightarrow -m_3$, there are two ways:

- m_3 may continue to remain along the z-axis, and its magnitude may pass through 0 to become $-m_3$. If this the case, **P** will remain fixed in the direction y, and **there is no direct coupling between m_3 and P**.
- It might be energetically more favorable to leave the magnitude of m_3 unchanged and its direction may rotate to $-z$;
- If this the case m_3 must rotate staying on the $y-z$ plane, to remain $\perp$ to **q** (whose direction fluctuations cost the crystalline anisotropy energy);
- Then to maintain the lowest energy configuration **P** reverses its direction to $-y$.

One more term can be added to Landau F_{ME}:

$$\mathbf{P}\gamma\nabla(\mathbf{M}^2)$$

It gives a surface contribution only when **P** is assumed to be independent of **r**. However the dependence of **P**(**r**) and **M**(**r**) need not be the same. Then for the phase dislocated, acentric SDW

$$M = M_0 \cos(q_m x + \phi)$$

if

$$\chi_E^{-1} = e_0 + e_1 \cos(qx)$$

Then

$$P = p_0 + p_1 \cos(qx)$$

Where

$$p_0 = -\frac{\gamma q_m M_0^2}{2} \frac{e_1}{2e_0^2 - e_1^2} \sin(2\phi)$$

$\mathbf{M}^2$ is by itself inversion invariant. It is lagging behind the P. Thus $\mathbf{M}^2$ has a directionality relative to P.

This works if:

$$q_m = \frac{q}{2}$$

Polarization vanishes for the case that q_m is incommensurate.

More general Weak crystallization:

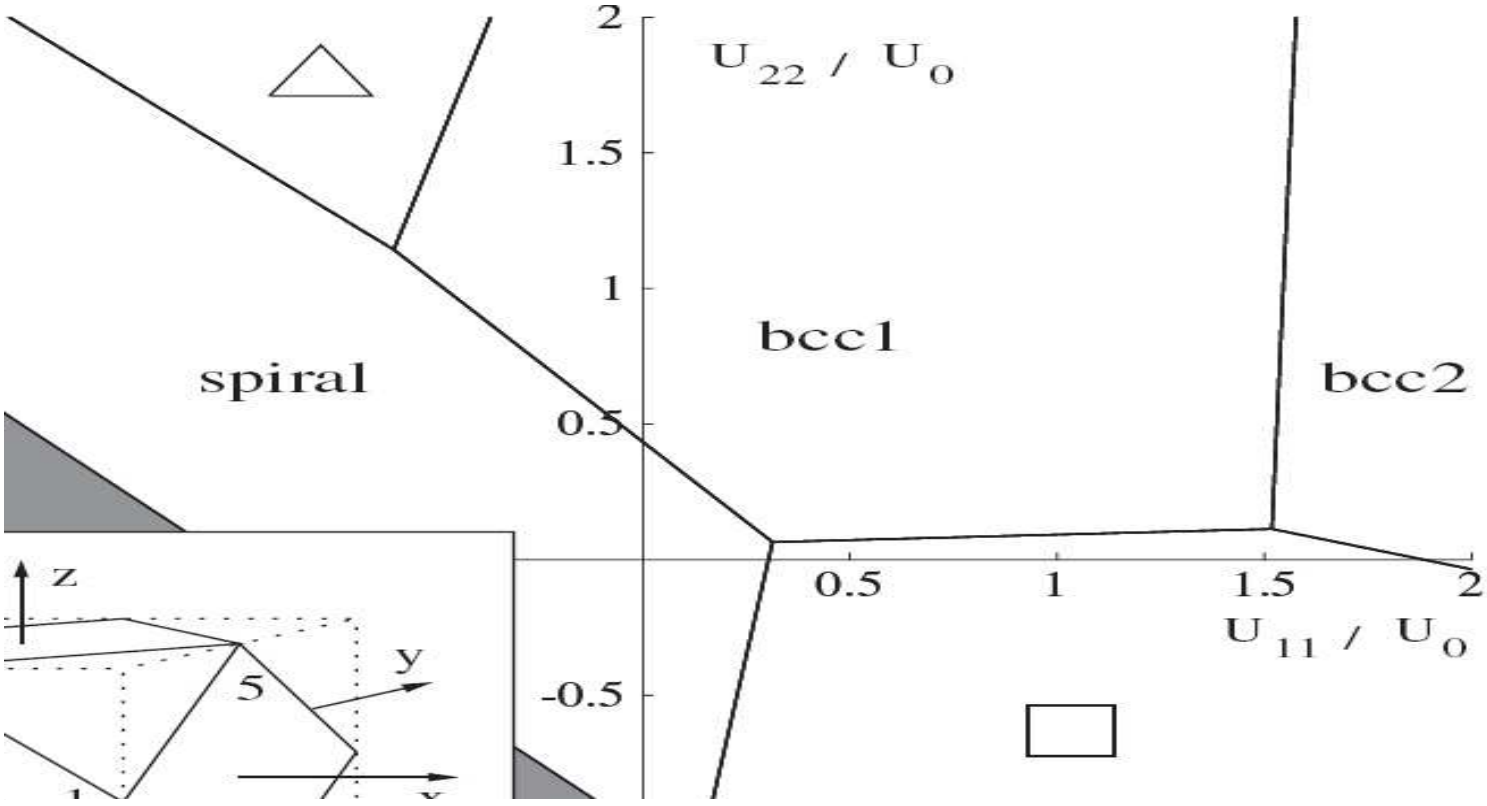

Figure: Mean fi eld phase diagram of the 6-mode model.

$$U(\theta,\phi) = U_0 + U_{11}\sin(\theta)\cos(\phi) + U_{20}(3\cos^2\theta - 1) + U_{22}\sin^2\theta\cos(2\phi)$$

Cycloidal magnetic ordering:

$$\mathbf{M_c}(\mathbf{r}) = (m_1 \cos(qx)\,,\, m_2 \sin(qx)\,,\, m_3)$$

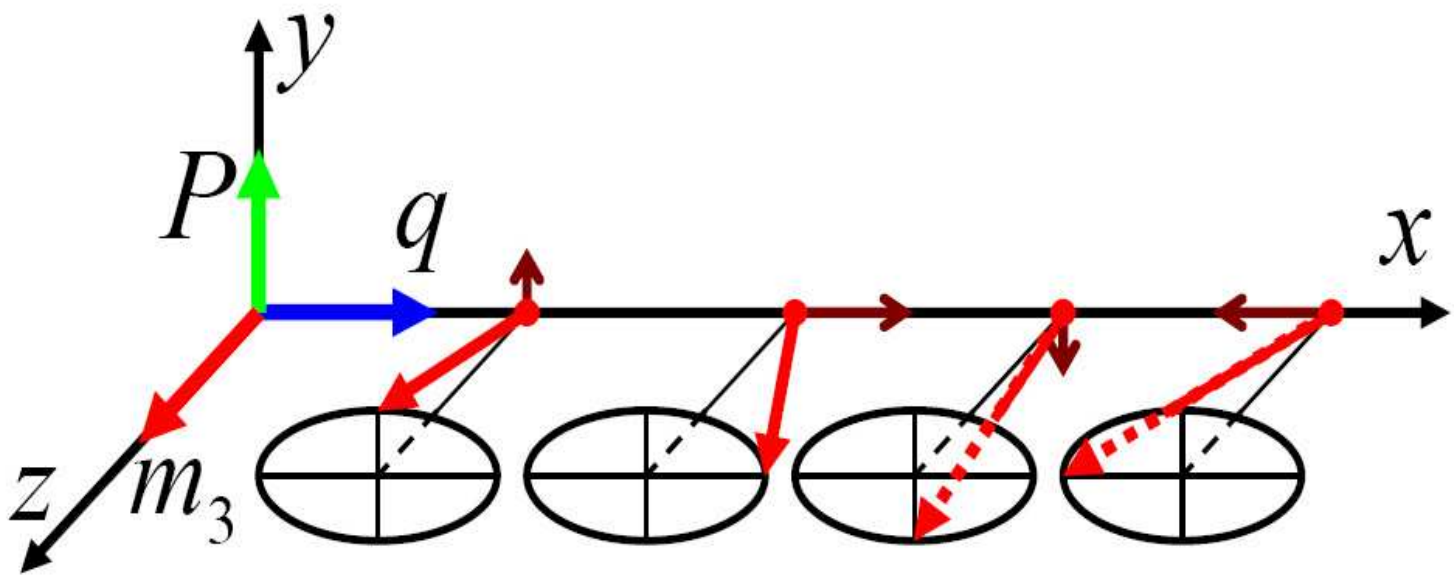

Figure: Conical cycloid structure.

Magnetic Goldstone modes:

$$\mathbf{M}(\mathbf{r}) = (m_1 \cos(qx + \phi(r)), m_2 \sin(qx + \phi(r)), m_3)$$

The elastic energy for this fluctuation cannot involve $(\partial_y \phi)^2$, $\partial_z \phi)^2$, while it must involve the longitudinal component $\partial_x \phi)^2$. This is because a uniform rotation of **q** ($\phi(r) \propto ay + bz$ must not cost any energy.
Generic fluctuations above the saddle point solution M_c include:

- ϕ - fluctuation of **q**;
- δ_y and δ_z - rotation of the cycloidal plane and m_3 about the y and the z axes, respectively (for the circular cycloidal state, $m_1 = m_2$, δ_z renormalizes ϕ);
- δ_x describes the rotation of the cycloidal plane about the pitch vector itself.

Generic fluctuation of M:

$$\delta\mathbf{M}(\mathbf{r}) = \begin{pmatrix} -m_3\delta_y - (\phi m_1 + \delta_z m_2)\sin(qx) \\ -m_3\delta_x + (\phi m_2 + \delta_z m_1)\cos(qx) \\ \delta_y m_1 \cos(qx) + \delta_x m_2 \sin(qx) \end{pmatrix}$$

The true Goldstone mode is a linear combination of ϕ, δ_y and δ_z, to linear order in p:

$$\alpha = \phi(p) + i\frac{p_z}{q}\delta_y(p) + i\frac{p_y}{q}\delta_z(p)$$

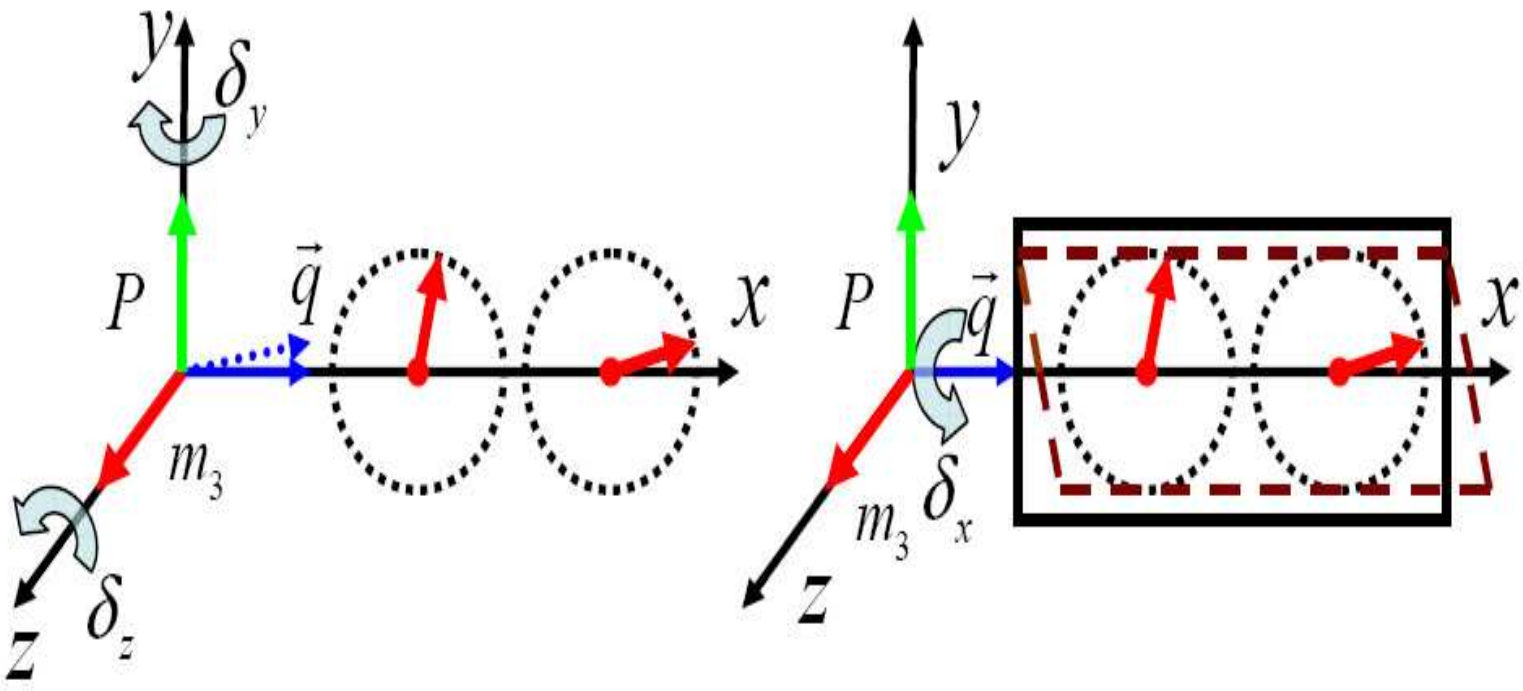

Figure: Goldstone mode α.

Two cycloidal Goldstone modes:

$$\omega_0 = 2(m_1^2 + m_2^2)q^2 p_x^2$$

As expected, there is no contribution from p_y, p_z at this order. The other Goldstone mode is δ_x with the momentum space dispersion relation starting at the order p_x^2, p_y^2, p_z^2.

- In the presence of lattice and spin anisotropies, the foregoing results are valid only above the anisotropy energies;
- The mode α depends quadratically on all p_i below the lattice anisotropy energy. However it continues to remain a Goldstone mode because of the broken translational symmetry. **This cycloidal magnon is analogous to the phonon mode in a crystal;**
- The other Goldstone mode δ_x acquires a gap given by the spin anisotropy below the weak spin anisotropy energy.

Goldstone mode correlation functions:

$$C_{\alpha\alpha}(p) = \frac{\sum_i \eta_i p_i^2}{\Delta(p)}$$

$$C_{\delta_x \delta_x}(p) \propto \frac{q^2 p_x^2}{\Delta(p)}$$

$$C_{\alpha \delta_x}(p) \propto \frac{p_x p_z}{\Delta(p)}$$

where $\Delta(p) \propto p_x^2 \sum_i \beta_i p_i^2$

Magnetic susceptibility:

$$\chi_{xx} \propto m_3^2 \frac{p_z^2}{q^2} C_{\alpha\alpha}(\mathbf{p}) + \frac{1}{4} m_1^2 (C_{\alpha\alpha}(\mathbf{p}-\mathbf{q}) + C_{\alpha\alpha}(\mathbf{p}+\mathbf{q})$$

It follows that the susceptibility functions diverge both at $p = 0$ and $p = \pm q$ for the conical cycloid state, the divergence at $p = 0$ originating from m_3. When $p \to q$ along p_x all χ_{ii} diverge as $(p_x - q)^{-2}$, whereas when $p \to q$ along y or z directions, χ_{xx} and χ_{yy} scale as p_i^{-4}, and χ_{zz} scales as p_i^{-2}.

Polarization correlations:

The correlation functions transverse to **P** diverge near $p = 0$ and $p = q$:

$$< P_z(p) P_z(-p) > \propto p_i^{-2}$$

(δ_x Goldstone mode).

$$< P_x(p) P_x(-p) > \propto p_y^{-2}$$

(α Goldstone mode). In the conical cycloid state (**but not in the ordinary cycloid state!**) the polarization correlation functions diverge also near $p = q$ but these electromagnon fluctuations will be difficult to see in optical experiments (non-zero momentum).

Landau model with DM (antisymmetric) and exchange (symmetric) M.E. couplings:

- Magnetic free energy:

$$F_M = \frac{a}{2}M^2 + \frac{b}{4}M^4 + \frac{1}{2}\sum_i M_i \hat{L}_i M_i$$

  where

$$a + \hat{L}_i \simeq \alpha_i + c_x \nabla_x^2 + c\nabla_\perp^2$$

- Dynamics

$$\dot{\mathbf{M}} = \gamma \mathbf{M} \times \mathbf{H}_{eff}$$

  where $\mathbf{H}_{eff} = (\hat{L}_x M_x\ ,\ \hat{L}_y M_y\ ,\ \hat{L}_z M_z)$

- If a, b, $c > 0$ the system shows no instability with respect to uniform magnetization.
- If $\alpha_x < \alpha_y < \alpha_z$ LSDW occurs when $\alpha_x < 0$, and $\alpha_y > 0$.
- For P.C. $\alpha_x < 0$, and $3\alpha_x \leq \alpha_y \leq \alpha_x/3$ with $\alpha_z > a$ in both cases.

Low-lying magnetic modes in LSDW:

$$\omega_{y/z} = 2m_x^2(\alpha_{z/y} - \alpha_x + c_x q_x^2 + c q_\perp^2)(-\alpha_x + c q^2)$$

at $q \to 0$, and

$$m_x^2(\tilde{\alpha}_{z/y} - 2\alpha_x + c(q')^2)(\alpha_{y/z} - \alpha_x + c_x (q'_x)^2 + c(q'_\perp)^2)$$

at $q - Q \to 0$ ($m_x = \gamma m_1/2$ and
$\hat{L}_i \exp(\pm i2Qx) \equiv \tilde{\alpha}_i \exp(\pm i2Qx)$).

- Closer the transition is, the smaller is the gap at $q \to 0$. On the contrary, the gap at $q \to Q$ is not sensitive to α_x.
- Similar expressions for TSDW (replacing y and x).
- For P.C. ω_z^2 is the sum for LSDW and TSDW.

Tera-Hertz study of electromagnon in $TbMnO_3$:

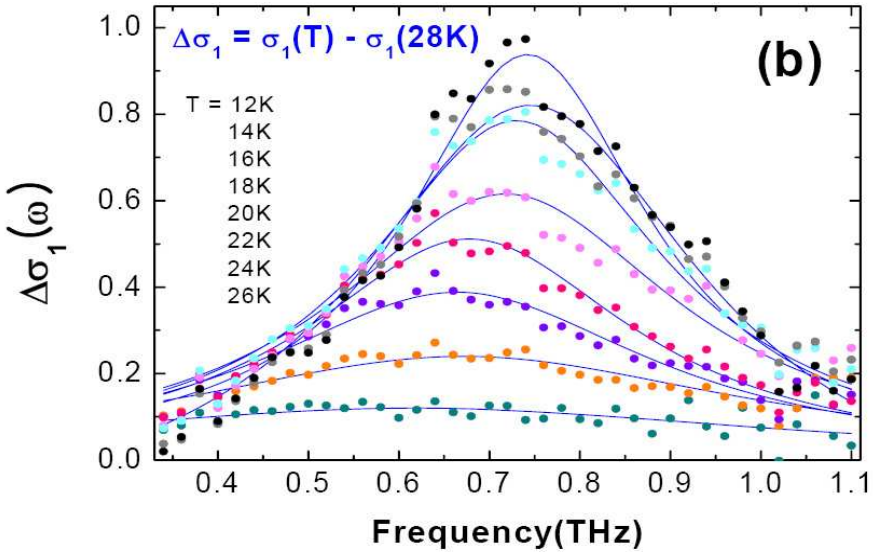

Optical response with light polarized within cycloidal plane contains no magnetic anomaly (only bare optical phonon frequencies). In the light polarized along the normal the AC susceptibility has two poles at shifted phonon and AF frequencies. Even though the AC electric field is $q = 0$ excitation, it couples to $q \neq 0$ magnons.

Generation of P by H in $ZnCr_2Se_4$:

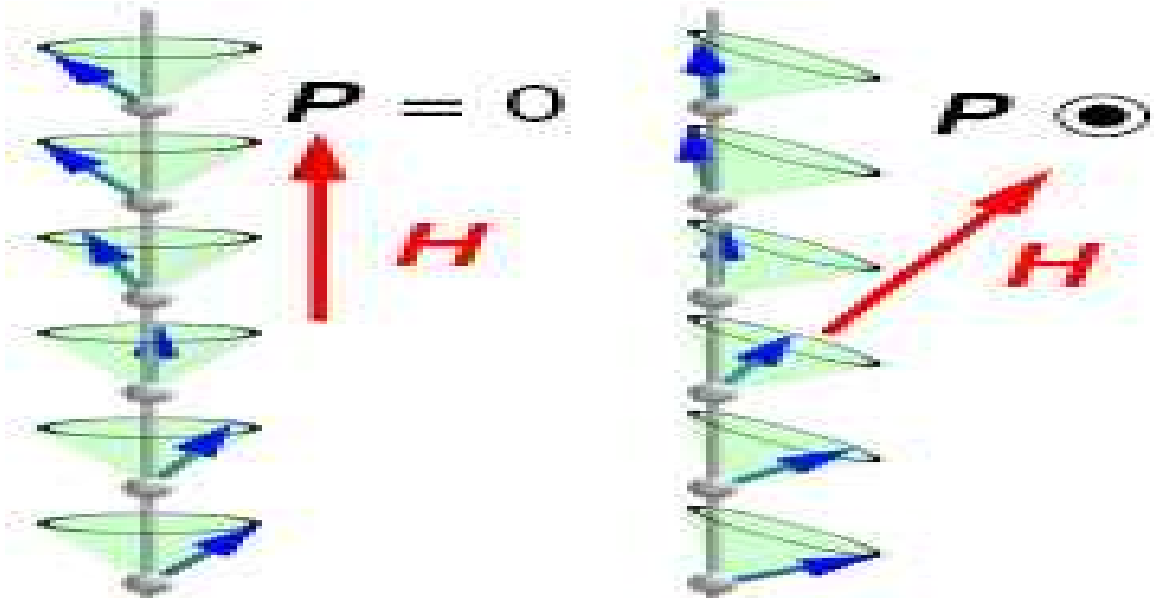

Under the **H** applied parallel to (100) direction, spin forms the longitudinal conical spiral, and $\mathbf{P} = 0$. When **H** is not parallel to the spiral axis, the cone is tilted and $\mathbf{P} \neq 0$ and is perpendicular to both, the cone axis and the spiral axis.

H-dependence of the electric polarization in $ZnCr_2Se_4$:

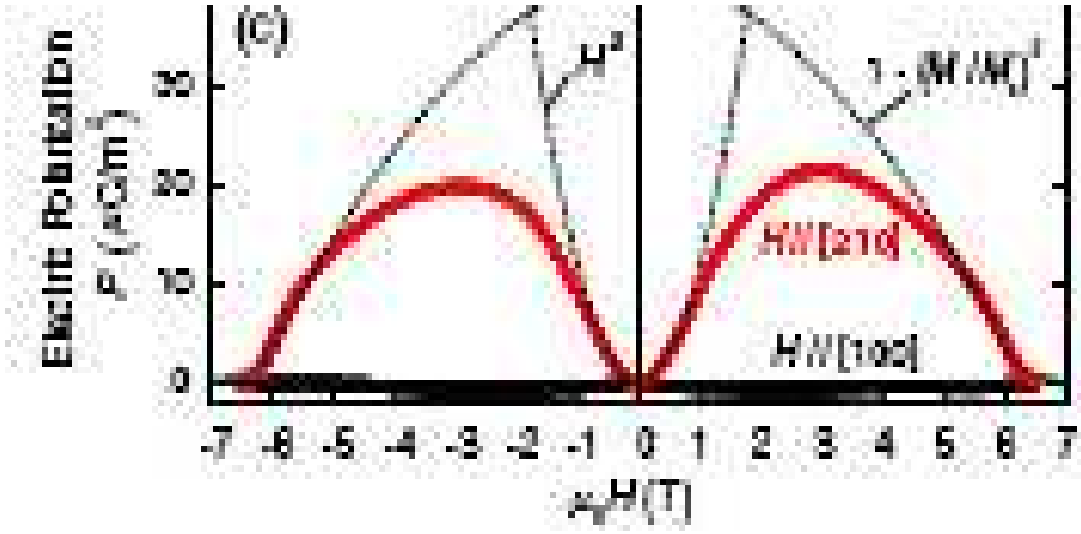

In the low H region, the P is governed by the tilting of the helical plane and $\propto H^2$. In the high H region it is governed by the closing cone angle and the P is expected to be $\propto [1-(M/M_s)^2]$, where M_s is the saturated magnetization.

Materials - possible candidates:

- Cubic spinel oxide $CoCr_2O_4$;
- Perovskite $RMnO_3$ (where $R = Tb, Gd$);
- Cobaltite, $BaCo_2(AsO_4)_2$
- RMn_2O_5 (if $R = Y$ - acentric SDW).

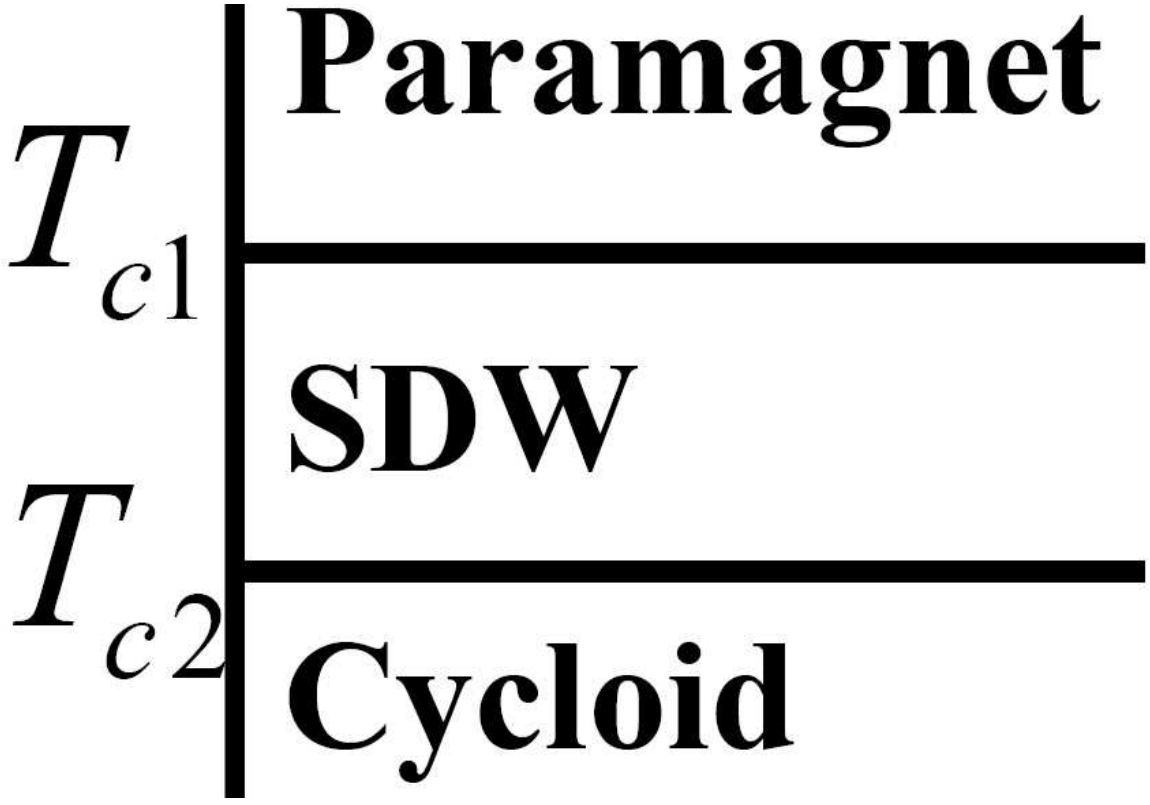

$MnWO_4$ multiferroic:

For decoupled spin and coordinate space, the energies of helical and cycloidal modulations are identical. However if spins are constrained to lie on a plane, and lattice anisotropy forces **q** to be also on that plane - the energy of the cycloidal modulation is lower than that of the helical.

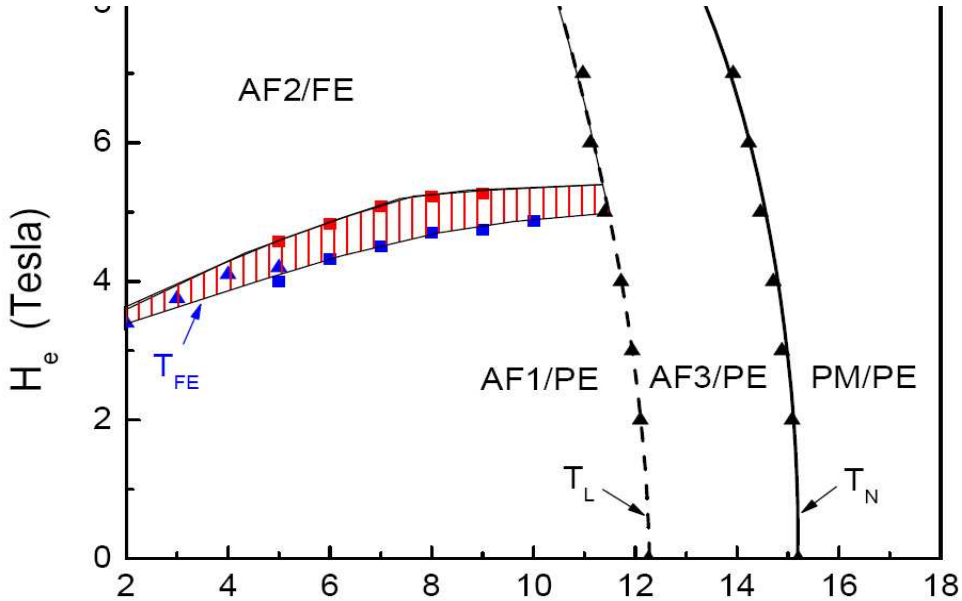

0.1 *Fe* substitution suppresses F.E. (it increases the uniaxial anisotropy), but it is restored in a magnetic field along the easy axis (because it restores a helical spin structure).